

# Effect of rhenium addition on fracture toughness of tungsten at elevated temperatures

Y. MUTOH, K. ICHIKAWA

*Nagaoka University of Technology, Nagaoka-shi 940-21, Japan*

K. NAGATA

*Toshiba Co., Tsurumi-ku, Yokohama-shi 230, Japan*

M. TAKEUCHI

*Honda UK, Manufacturing Ltd, Swindon, Wiltshire, SN3 4TJ, UK*

Fracture toughness tests of tungsten and tungsten–rhenium alloy specimens were carried out at elevated temperatures. Temperature dependence of fracture toughness and effect of rhenium content on fracture toughness were investigated. Although fracture toughnesses of three kinds of specimens with rhenium contents of 0, 5 and 10 wt% were almost identical at room temperature, fracture toughness at elevated temperatures increased with increasing rhenium content. The brittle–ductile transition, similar to steels, and subsequent transition of the fracture mode from ductile dimple to intergranular were observed for all three kinds of specimens. With increasing rhenium content, the transition temperatures increased. A significant grain growth was found, not for tungsten–rhenium alloy specimens, but for a tungsten specimen without rhenium in a temperature range higher than the recrystallizing temperature, which resulted in transition of the fracture mode from dimple to intergranular.

## 1. Introduction

An increase in demand for tungsten for aerospace and nuclear industries has recently become noticeable. This is due to the attractive properties of tungsten, such as a high melting point (approximately 3410 °C) and excellent mechanical properties at high temperatures. At low temperatures tungsten is known as a poor toughness material, with high yield strength, low elongation and low reduction of area. At high temperatures it is embrittled by crystal growth due to recrystallization. Therefore, the ductility and brittleness of tungsten needs to be improved for its application as a structural material.

The ductility of tungsten W can be improved by removing the impurities in the grain boundaries and/or by fining the grain size. For this purpose, VIIa group elements, such as rhenium (Re) and technetium (Tc); VIII group elements, such as ruthenium (Ru) and osmium (Os), including elements such as titanium (Ti) and cobalt (Co), are added to tungsten [1, 2]. Particularly, Re reduces the ductile–brittle transition temperature and significantly improves ductility. Garfinkle *et al.* found that the addition of Re by 25 wt% (tungsten–25% Re alloy) increased ductility by 260% at 2000 °C [3]. However, the fundamental characteristics of tungsten and its alloys, such as temperature dependencies of strength and fracture tough-

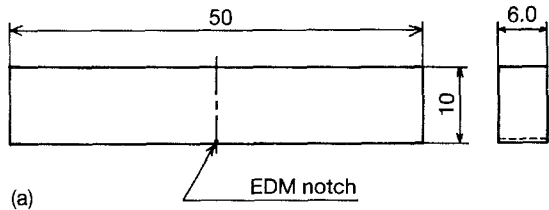
ness and fracture mechanisms at high temperatures, have not been investigated.

In the present study, temperature dependence of fracture toughness and fracture mechanisms in tungsten and tungsten–rhenium alloys were investigated in detail. The effect of rhenium addition on fracture toughness was also discussed.

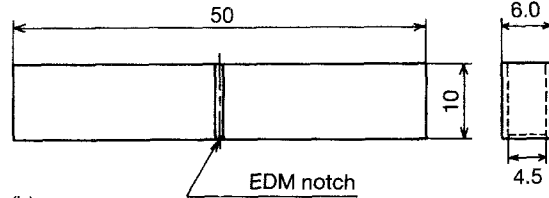
## 2. Experimental procedure

The materials used for the tests were 99.9% W–0.04% Fe alloy (W), where Fe is a sintering additive, 95.0% W–5.0% Re alloy (W–5 Re), and 90.0% W–10.0 Re alloy (W–10 Re). Fig. 1 shows the details of the specimens employed in toughness tests. Standard (non-sidegrooved) and sidegrooved specimens were tested. The details of the electric discharge machined (EDM) notch and sidegroove are also shown in the figure. The sidegroove was made to be  $(B - B_N)/B = 0.25$ , where  $B$  and  $B_N$  are the nominal and the net thickness of the specimen, respectively, by machining with a precision cutting tool after the introduction of precrack by the bridge indentation method (BI method) [4, 5].

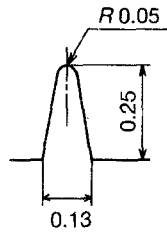
Fig. 2 shows the BI method for introducing precrack with a span length of 7 mm. A brittle precrack was initiated when the compression load became approximately 120 kN. The length of the introduced



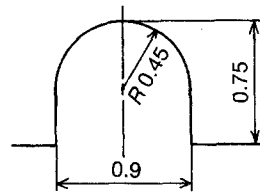
(a)



(b)



(c)



(d)

Figure 1 Fracture toughness specimen: (a) standard, (b) sidegrooved, (c) detail of EDM notch, and (d) detail of sidegroove.

precrack was 4–6 mm, namely  $a/w = 0.4–0.6$  ( $a$ , crack length; and  $w$ , specimen width). The precrack length was determined as the mean value of three points, which were measured at equal spans in the direction of the specimen thickness after the specimen was fractured [6]. The precrack introduced was sharp and linear, as shown in Fig. 3.

Three point bending fracture toughness tests were carried out according to ASTM E399 with an Instron type universal test machine in the range from room temperature to 1600 °C. The span length was 40 mm and the crosshead speed was 0.5 mm min<sup>-1</sup>. A vacuum electric furnace was employed for the high temperature tests. The specimen was tested after soaking for 15 min at the test temperature. During the test the vacuum in the furnace was 2.6 ~ 6.6 mPa and the temperature was maintained at  $\pm 3$  K.

It is possible to determine plane-strain fracture toughness  $K_{IC}$  of tungsten at low temperatures, since tungsten is a brittle material at low temperatures. The value of  $K_{IC}$  was determined for the standard specimen shown in Fig. 1a using the following equations [6]

$$K_{IC} = \sigma_f (\pi a)^{1/2} f(\xi)$$

$$\sigma_f = 3P_f S / 2w^2 B$$

$$f(\xi) = [1.99 - \xi(1 - \xi)(2.15 - 3.93\xi + 2.7\xi^2)] / \times [(\pi)^{1/2}(1 + 2\xi)(1 - \xi)^{3/2}] \quad (1)$$

where  $\xi$  is  $a/w$ ,  $B$  the thickness of the specimen,  $S$  the span length, and  $P_f$  the fracture load. At high temperatures the elastic-plastic fracture toughness  $J_{IC}$  value was determined by the convenient  $J_{IC}$  test method

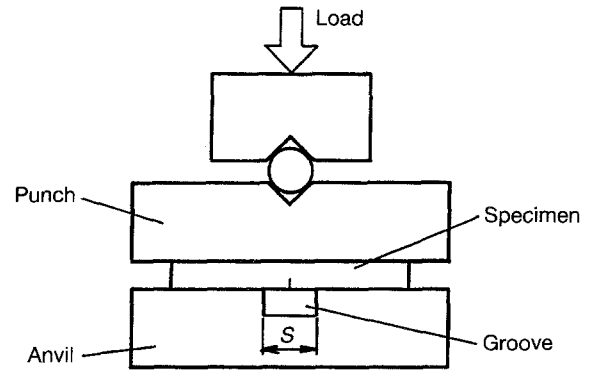


Figure 2 Precracking by the BI method.

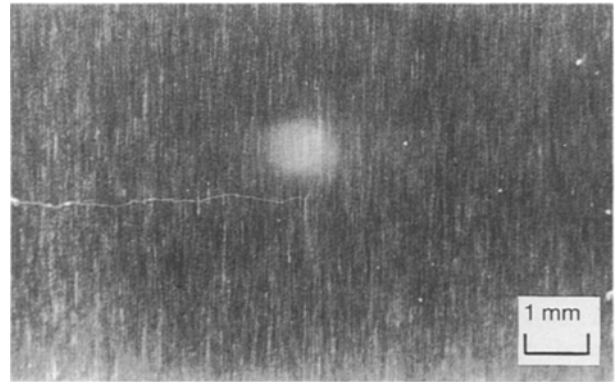


Figure 3 Precrack morphology.

[7, 8], because the  $K_Q$  value could not satisfy ASTM E399 requirements for a valid  $K_{IC}$ , and the fracture toughness could not be evaluated by the  $K_{IC}$  value. In the convenient  $J_{IC}$  test method used, the proper length of precrack and depth of sidegroove are introduced to coincide the stable crack initiation point with the maximum load point; and the  $J_{IC}$  value is evaluated from the maximum load point. The  $J_{IC}$  value was obtained from the following equation using the sidegrooved specimen shown in Fig. 1a

$$J_{IC} = 2A/B_e b \quad (2)$$

where  $A$  is the area under the load–displacement curve up to the maximum load point, and  $b$  the ligament length,  $B_e$  the effective thickness of the sidegrooved specimen [ $= (B \times B_N)^{1/2}$ ] [9]. Since the displacement at loading point could not be measured directly in a vacuum furnace at high temperatures, the displacement of the loading rod measured outside of the furnace was reduced by subtracting the displacement due to the elastic compliance of the test system. The sufficiently high accuracy of the reduced displacement was confirmed by a three point bend test of a rectangular beam without precrack, where the reduced displacement of the beam agreed well with that estimated based on the elastic beam theory.

Hardness measurement and microstructure observation were carried out on specimens which were kept at elevated temperatures for 15 min and then naturally cooled in the furnace, as well as the as-received specimen. The dependency of the fracture toughness and fracture mode on the microstructure and hardness was investigated.

### 3. Results and discussion

#### 3.1. Temperature dependency of fracture toughness

Load–displacement curves for the materials W, W–5 Re and W–10 Re in the range of room temperature to 1600 °C are shown in Figs 4, 5 and 6, respectively. At room temperature, unstable fracture occurred in the range of the 5% offset line in all three materials. As the temperature increased, non-linear behaviour became significant. The load–displacement curves showed that the  $K_{IC}$  test, using the standard specimen which was shown in Fig. 1a, was effective at temperatures up to 600 °C. At temperatures over 700 °C, the  $J_{IC}$  tests were carried out on the sidegrooved specimen shown in Fig. 1b to evaluate fracture toughness, since elastic–plastic fracture behaviour became dominant.

The relationship between fracture toughness,  $K_{IC}$ , and temperature is shown in Fig. 7. At room temperature all three materials showed similar  $K_{IC}$  values, namely 12–14 MPa m<sup>1/2</sup>. However, at higher temperatures the effect of Re addition became significant. Re increased fracture toughness as the temperature increased. The fact that the fracture toughness of the material W–10 Re is higher than that of the material W–5 Re at all temperatures indicates that  $K_{IC}$  can be increased with increasing Re content. At room temperature, the  $K_{IC}$  value of the material W is somewhat greater than that of the material W–5 Re. This may be due to the difference in the forging ratio during the manufacturing of the specimens, which induces different levels of residual stress.

The relationship between fracture toughness,  $J_{IC}$ , and temperature is shown in Fig. 8. In the range of room temperature to 200 °C, the  $J_{IC}$  value of the material W was greater than those of the materials W–5 Re and W–10 Re. This may be due to the fact that, as shown in Figs 4, 5 and 6, the addition of Re significantly increases Young’s modulus and consequently specimen rigidity, in spite of the similar fracture load for all three materials. When the temperature exceeded 400 °C, the  $J_{IC}$  values of the materials W–5 Re and W–10 Re dramatically increased and became greater than that of the material W. When the temperature exceeded 800 °C, the  $J_{IC}$  value of the material W also dramatically increased. The dramatic increase in fracture toughness is due to the transition in fracture behaviour from unstable fracture to stable fracture, which is observed on steel as a brittle–ductile transition [10]. The result shown in Fig. 8 indicates that the addition of Re can reduce the brittle–ductile transition temperature and make the sharp transition behaviour broad.

Fracture toughness,  $J_{IC}$ , decreased at temperatures over 1000 °C for the materials W–5 Re and W–10 Re, and over 1200 °C for the material W. The reduction rate of  $J_{IC}$  was much greater for the material W than for the other two materials. It is noted that the higher the Re content, the greater the  $J_{IC}$  value over 1300 °C at which the reduction rate became small.

The  $J_{IC}$  value of the material W–5 Re was low at all test temperatures and significantly low around 1000 °C compared with those of the materials W and

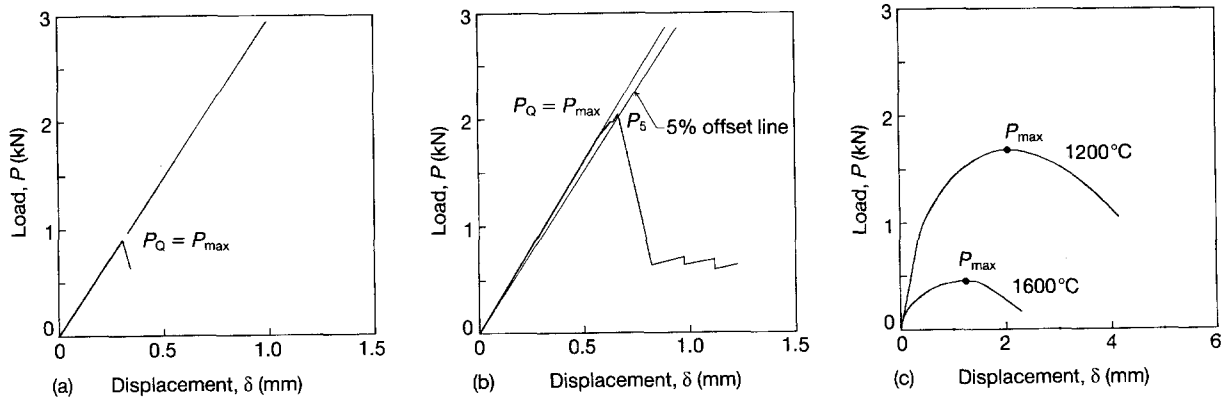


Figure 4 Load–displacement curves for W specimens: (a) standard at room temperature, (b) sidegrooved at 800 °C, and (c) sidegrooved at 1200 and 1600 °C.

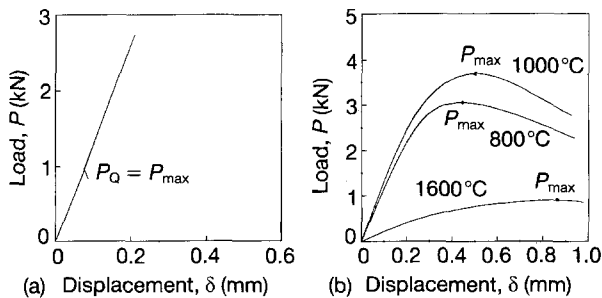


Figure 5 Load–displacement curves for W–5 Re specimens: (a) standard at room temperature, and (b) sidegrooved at 800, 1000 and 1600 °C.

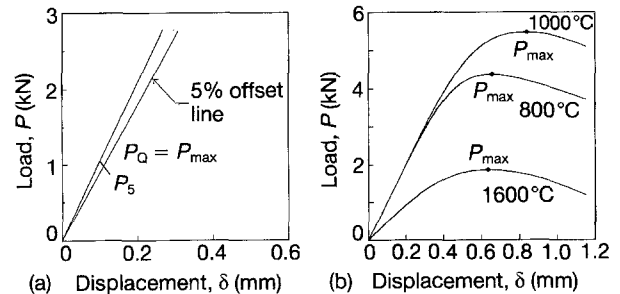


Figure 6 Load–displacement curves for W–10 Re specimens: (a) standard at room temperature, and (b) sidegrooved at 800, 1000 and 1600 °C.

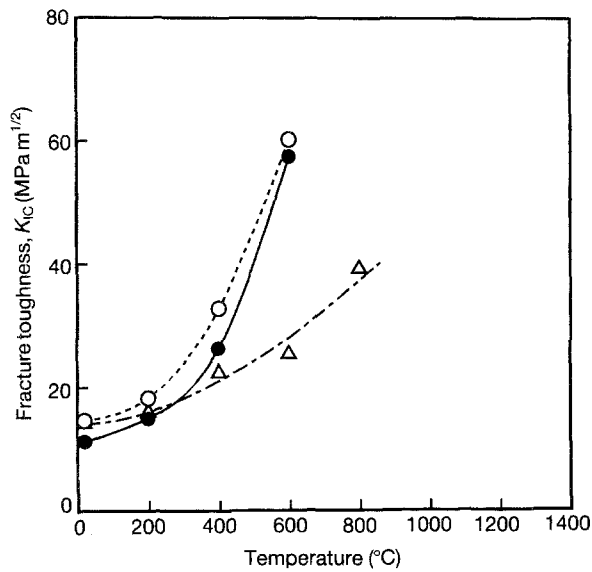


Figure 7 Temperature dependency of  $K_{IC}$  values for ( $\Delta$ ) W, ( $\bullet$ ) W-5 Re, and ( $\circ$ ) W-10 Re.

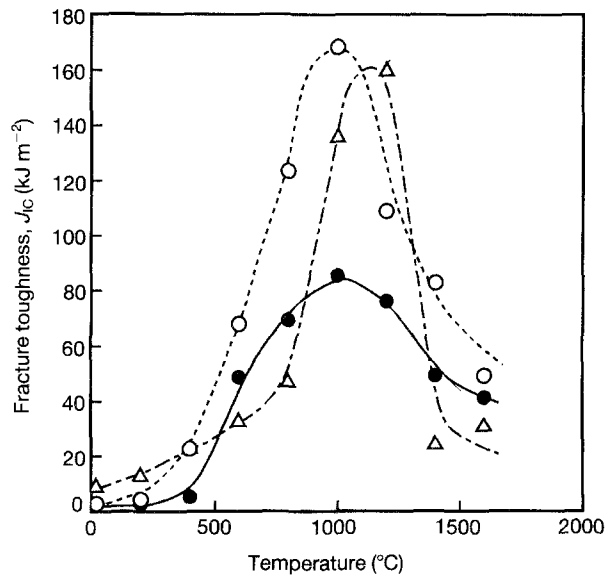


Figure 8 Temperature dependency of  $J_{IC}$  values for ( $\Delta$ ) W, ( $\bullet$ ) W-5 Re, and ( $\circ$ ) W-10 Re.

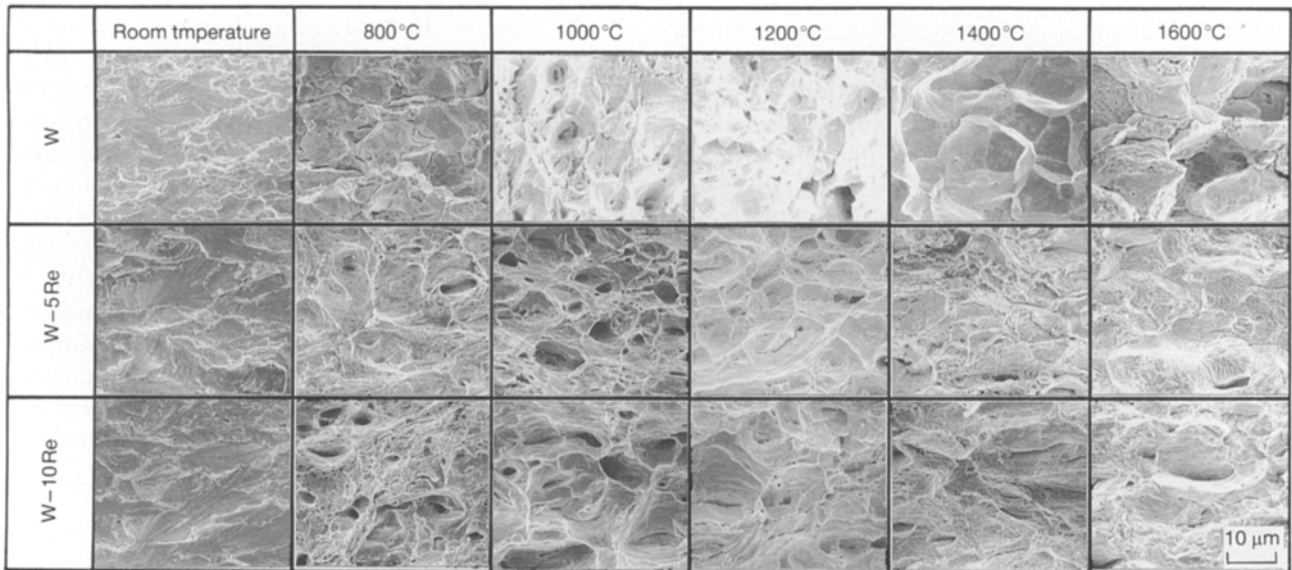


Figure 9 Fractographs.

W-10 Re. The reason for this, as can be understood from the load–displacement curves shown in Figs 4–6, is that Re added materials have a lower compliance in the elastic region and a lower deformation up to the maximum load,  $P_{max}$ , compared with the material W. On the other hand,  $P_{max}$  increases with the increase of Re content. Therefore, the  $J_{IC}$  values determined by the area under the load–displacement curve for the Re added materials become lower than that for the material W if the Re content is less than a certain critical level. It is noted that the critical level exists between 5 and 10% content Re.

### 3.2. Temperature dependency of fracture surface morphology

Fig. 9 shows the fracture surface near the precrack tip of specimens tested at room temperature, 800, 1000, 1200, 1400 and 1600 °C. At room temperature quasi-cleavage fracture, showing brittle fracture, is dominant

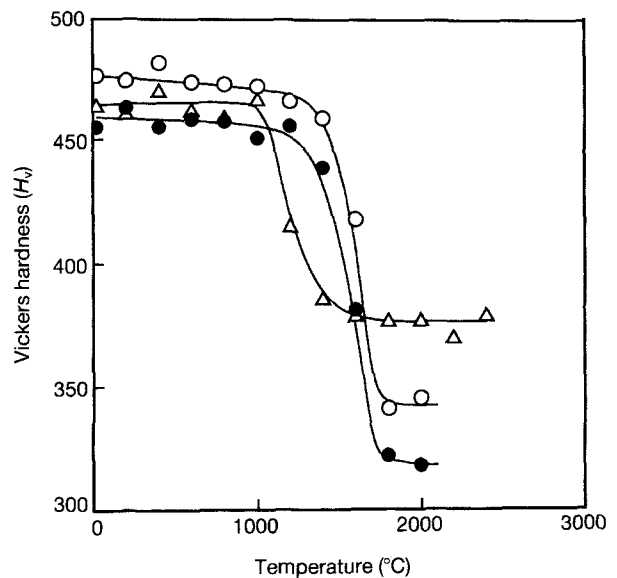


Figure 10 Relationship between hardness and holding temperature for specimens heated at various temperatures for ( $\Delta$ ) W, ( $\bullet$ ) W-5 Re, and ( $\circ$ ) W-10 Re.

in all three materials. At a temperature of 800 °C the fracture surfaces of the materials W-5 Re and W-10 Re show dominant dimple fracture, indicating that the brittle-ductile transition temperature is already exceeded. In the case of the material W, the fracture surface shows dominant quasi-cleavage fracture with increasing intergranular facets, but no dimple fracture is visible. The dominant quasi-cleavage fractures indicate that the transition from brittle fracture to ductile fracture has not occurred up to temperatures of 800 °C. These fractographical observations correspond to the facts that the transition temperature is reduced by the addition of Re, and that  $K_{IC}$  evaluation using a sidegrooved specimen is possible at a temperature of 800 °C for the material W. At temperatures over 800 °C dimple fracture, indicating ductile fracture, is dominant in all three materials. At a temperature of 1400 °C the fracture surface of the material W shows intergranular fracture, and the intergranular facets are much larger than those observed at temperatures under 800 °C. It is thought that the dramatic reduction of fracture toughness at temperatures over 1400 °C is due to crystal growth by recrystallization, resulting in the embrittlement of the intergranular region. In the case of materials W-5 Re and W-10 Re, dimple fracture is still a major fracture at a temperature of 1200 °C, and a mixture of dimple and intergranular fracture is visible at a temperature of 1400 °C. At a temperature of 1600 °C, material W-5 Re shows intergranular fracture, but significant crystal growth, observed in material W, is not noticeable. In the case of material W-10 Re, the fracture does not change to intergranular fracture at such a high temperature.

The result showing, that at temperatures over 1300 °C, the higher the Re content, the greater the  $J_{IC}$  value, is thought to be due to the fact that crystal

growth caused by recrystallization and embrittlement of the intergranular region at high temperatures, can be inhibited by the addition of Re.

### 3.3. Temperature dependency of hardness and microstructure

Although it is necessary to measure hardness and to observe microstructures at high temperatures, it was difficult in the present work. Therefore, the recrystallization temperature was estimated by the hardness and microstructural change in the specimens which were heated at certain temperatures for 15 min and were cooled down in the furnace. Fig. 10 shows the relationship between hardness and holding temperature for the specimen heated at various temperatures. The hardness of the material W dramatically decreased at around a temperature of 1200 °C. The transition temperature of hardness, which is 1200 °C, coincides with the temperature at which the  $J_{IC}$  value is dramatically reduced. Similar behaviour of the change in hardness was observed for both materials W-5 Re and W-10 Re. The transition temperature of hardness increased with increasing Re content. This result coincides with the observation that the higher the Re content, the higher the transition temperature from transgranular fracture to intergranular fracture.

Fig. 11 shows microstructures of the materials heated at various temperatures. Significant crystal growth was observed at a temperature of 1600 °C for material W, but not significant for the materials W-5 Re and W-10 Re. This result coincides with the results of toughness tests and fracture surface observation. Electron probe X-ray microanalysis (EPMA) examination showed that the Re was not segregated in the grain boundary, but uniformly distributed in the W granulars.

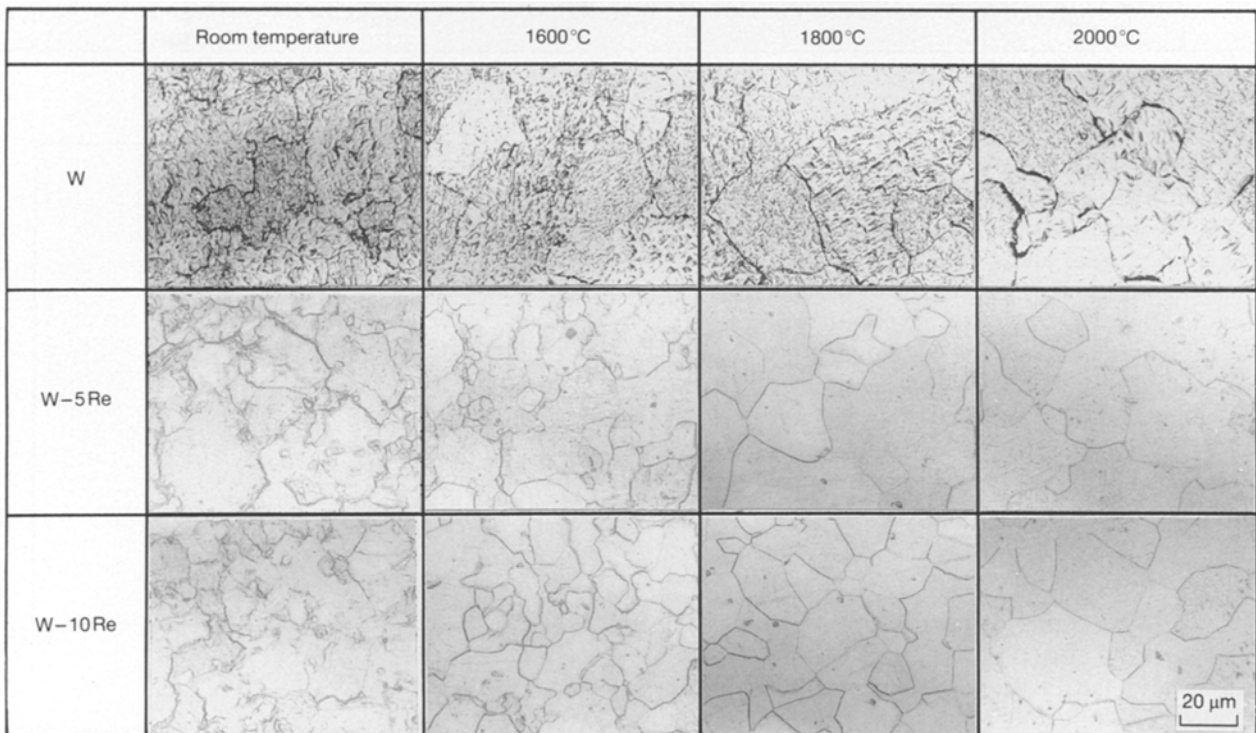


Figure 11 Microstructure of specimens heated at various temperatures.

#### 4. Conclusions

Fracture toughness tests were carried out in the range of room temperature to 1600 °C using tungsten alloys, with the addition of Re to improve high temperature toughness of tungsten. The following conclusions can be summarized from the present work.

1. A brittle-ductile transition was observed at 900 °C in material W, and at 600 °C in materials W-5 Re and W-10 Re. The brittle-ductile transition temperature was reduced by the addition of Re. Brittle unstable fracture occurred at temperatures lower than the transition temperature in all materials, and the unstable fracture was quasi-cleavage fracture. At temperatures higher than the transition temperature, ductile fracture due to dimple fracture occurred.

2. For material W, when the temperature exceeded 1200 °C, crystal growth due to recrystallization and the embrittlement of the intergranular region occurred, and the fracture toughness value decreased dramatically due to intergranular fracture. For materials W-5 Re and W-10 Re, no significant recrystallization and embrittlement were observed, and the reduction of toughness was not so severe as in the case of the material W. In this temperature range the greater the Re content, the higher the fracture toughness. For material W-5 Re intergranular fracture became dominant when the temperature reached 1600 °C. How-

ever, material W-10 Re still showed transition fracture mode, with transgranular and intergranular fracture facets, at a temperature of 1600 °C.

#### References

1. Y. FUKASAWA and S. OGURA, *Sosei-to-Kako* **19** (1987) 286.
2. G. V. SAMSONOV and R. A. ALFINTSEVA, *Poroshkovaya Metallurgiya* **110** (1972) 19.
3. M. GARFINKLE, W. R. WITZKE and W. D. KLOPP, *Trans. AIME* **245** (1969) 303.
4. T. SADAHIRO and S. TAKATSU, *Modern Develop. Powder Metall.* **14** (1981) 501.
5. Y. MUTOH, K. TANAKA and N. MIYAHARA, *Trans. Jpn. Soc. Mech. Eng.* **55** (1989) 2144.
6. ASTM Standard E399-1981 (American Society for Testing Materials, Philadelphia, PA).
7. Y. MUTOH, "Role of Fracture Mechanics in Modern Technology", edited by G. C. Sih, H. Nishitaki and T. Ishihara, (Elsevier Science Publishers, North Holland, 1987) p. 503.
8. *Idem*, in "Proceedings of International Conference on Evaluation of Materials Performance in Severe Environments", (ISIJ, Tokyo, 1989) p. 695.
9. Y. MUTOH, I. SAKAMOTO and S. TAKEDA, *JSME Int. J.* **32** (1989) 432.
10. D. BROEK, "Elementary Engineering Fracture Mechanics", (Noordhoff, Leyden, 1974) Chapter 1.

*Received 9 September 1993  
and accepted 6 July 1994*